DINAME 2017 - Proceedings of the XVII International Symposium on Dynamic Problems of Mechanics
A. T. Fleury, D. A. Rade, P. R. G. Kurka (Editors), ABCM, São Sebastião, SP, Brazil, March 5-10, 2017

Use of Piezoelectric Materials in Energy Harvesting Systems as Sensors and Actuators

Aline S. De Paula[1], Marcelo A. Savi[2], Wescley O. V. Barbosa[1], Tiago L. Pereira[1], Adriano T. Fabro[1]

[1]Universidade de Brasilia, Department of Mechanical Engineering, 70.910.900 - Brasília - DF, Brazil, alinedepaula@unb.br

[2]Universidade Federal do Rio de Janeiro, COPPE - Department of Mechanical Engineering, Center for Nonlinear Mechanics, 21.945.972 - Rio de Janeiro - RJ, Brazil, savi@mecanica.ufrj.br

Abstract: This work exploits the idea of using piezoelectric materials as sensors and actuators in energy harvesting systems. The main objective of these systems is the vibration-based energy harvesting where available mechanical energy is converted into electrical energy. In this regard, piezoelectric materials are employed to establish a mechanical-electrical conversion. The harvested energy from harmonically excited linear system achieves its best performance when it is excited in its fundamental resonance. If the excitation frequency is changed slightly, the power output is drastically reduced. Thus, there are research efforts focused on the concept of broadband energy harvesting to overcome this drawback. An interesting alternative is to explore nonlinear bistable energy converters. The search for broadband energy harvesters includes harmonic and randomly excited system. This paper deals with energy harvesting using a bistable nonlinear piezomagnetoelastic structure. Initially, random vibrations are investigated and a condition for energy harvesting enhancement is established. Afterward, the same structure is analyzed under harmonic and random excitations. The goal is to present an investigation of the best electrical output response of the system. It is proposed a methodology to evaluate the system performance when both harmonic and random excitations are considered together. Finally, the use of piezoelectric materials as sensors and actuators is incorporated in the system considering the structure subjected to harmonic excitation. The actuator is considered for control purposes, exploiting chaos control techniques with two different goals: vibration reduction, where vibration amplitudes should be reduced; and energy harvesting, where large amplitude responses are exploited to generate energy. In both situations, chaos control is simultaneously employed with vibration energy harvesting. Both control actuation and energy harvesting are induced employing piezoelectric materials. In the case of vibration reduction, the goal is that the controller can use the harvested energy. In the case of energy harvesting, the control is used to obtain a better performance of the device.

Keywords: Piezoelectric materials, energy harvesting, chaos control, sensors, actuators

INTRODUCTION

Energy is essential for human life being a critical point in contemporary world. Fossil fuels are established as the main source of energy, but the growing necessity to deal with environmental issues is pushing changes to renewable energy sources. In the regard, several challenging researches are being carried out looking for alternatives related to energy.

Energy harvesting is a concept where different forms of available environmental energy are converted through electrical, useful energy. Usually, available energy can be related to sea waves, wind, solar, among other forms. An interesting alternative is the vibration energy that can be associated with different kinds of structures, airplanes, oil drilling, boats, roads, human movements, micro-electro-mechanical devices, among several others.

Piezoelectric vibration-based energy harvesting is an interesting alternative to be exploited in different possibilities. The essential idea is to convert available mechanical vibration into electrical energy using piezoelectric elements. The harvested energy can be used to recharge batteries or to perform a specific task. Control is a possibility where the system can generate the controller energy. In this regard, piezoelectric elements can be employed both as sensor and actuator.

Vibration-based energy harvesting using piezoelectric elements is an active research area nowadays. The main challenge is to improve the harvesting capacity, enhancing system efficiency. An archetypal model to describe energy harvesting system is represented by a mechanical oscillator connected to an electrical system through a piezoelectric element. Mechanical, electrical and piezoelectric nonlinearities can be exploited to enhance system efficiency. Besides, random effects need to be investigated in order to evaluate system performance. Mechanical nonlinearities are usually associated with bistable systems represented by Duffing oscillator (Cottone *et al.*, 2009; Shahruz, 2008; Erturk at al., 2009).

This paper deals with a bistable nonlinear piezomagnetoelastic structure employed for energy harvesting purpose. Mathematically, an electro-mechanical oscillator represents the system. Initially, the analysis of the harvested energy of the system subjected to random, and random-harmonic excitations are treated. In the first case the aim is to establish a condition of energy harvesting enhancement of the nonlinear system when compared to the linear one. Afterward, it is exploited the idea to use piezoelectric materials as sensors and actuators. In this case, the structure is subjected to harmonic excitation and energy harvested is employed to control purposes with two different goals: vibration reduction, where vibration amplitudes should be reduced; and energy harvesting, where large amplitude responses are exploited to generate energy. Harvested energy is used to supply the power (partially or fully) of the actuator. Chaos control methods are employed considering two approaches: the Extended Time-Delayed Feedback method (ETDF) (Socolar et al., 1994); the Semi-Continuous (SC) chaos control method proposed by Hübinger et al. (1994). Results of numerical simulations provide a general idea about energy harvesting capacity considering different potential applications.

PIEZOMAGNETOELASTIC STRUCTURE

The energy harvesting system is a magnetoelastic structure that consists of a ferromagnetic cantilevered beam with two permanent magnets, one located in the free end of the beam and the other at a vertical distance *d* from the beam free end, subjected to base excitation. In order to use this device as a piezoelectric power generator, two piezoceramic layers are attached to the root of the cantilever and a bimorph generator is obtained as depicted in Figure 1. The archetypal model is shown together with the structure, where $k(x)$ is the stiffness, c the linear viscous damping coefficient, R the electrical circuit resistance, i the current flowing into the circuit and θ and Cp the effective piezoelectric coefficient and capacitance, respectively.

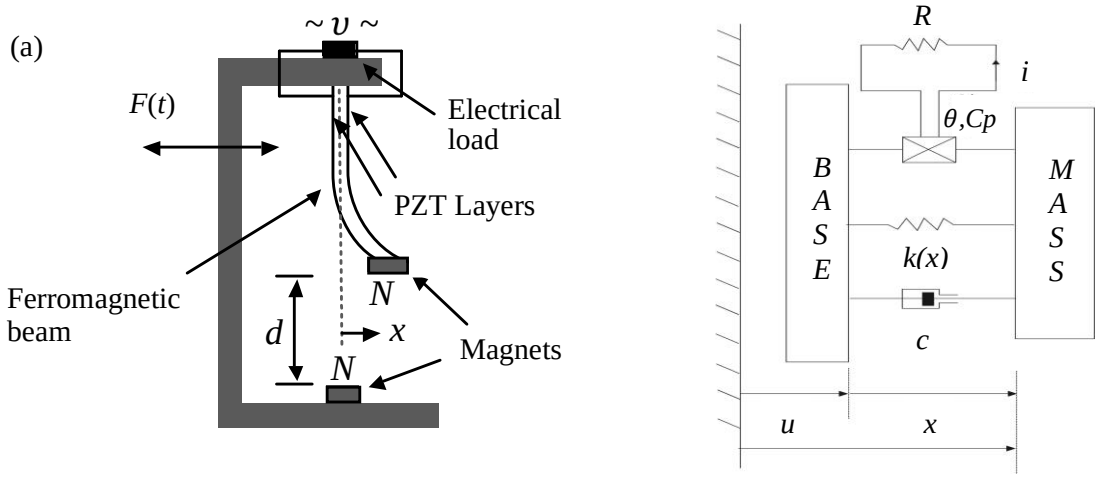

Figure 1 - Piezomagnetoelastic energy harvester schematic figure (De Paula et al., 2015).

The PZT layers are connected to an electrical load (a resistor for simplicity) and the voltage output of the generator across the load is the primary interest in energy harvesting. The electromechanical system behavior is approximated by the following equations of motion where x is the dimensionless tip displacement of the beam in transverse direction, ζ is the mechanical damping ratio and overdot represents differentiation with respect to dimensionless time. Erturk & Inman (2008,2009) and Erturk *et al.* (2008 and 2009) showed details of the formulation expressed by:

$$\ddot{x} + 2\zeta\dot{x} + \beta x + \alpha x^3 - \chi\upsilon = F(t) \tag{1}$$

$$\dot{\upsilon} + \lambda\upsilon + \kappa\dot{x} = 0 \tag{2}$$

where υ is the dimensionless voltage across the load resistance, χ is the dimensionless piezoelectric coupling term in the mechanical equation, κ is the dimensionless piezoelectric coupling term in the electrical circuit equation, λ is the reciprocal of the dimensionless time constant ($\lambda=1/R_lC_p$ where R_l is the load resistance and C_p is the equivalent capacitance of the piezoceramic layers), β defines the equivalent beam stiffness and magnet force, while α is defined uniquely by the magnet force. Note that, if $\beta<0$ the system is bistable with three equilibrium points: $(x_{SAD}, \dot{x}_{SAD}) = (0,0)$ (a saddle) and $(x_{SEP}, \dot{x}_{SEP}) = (\pm\sqrt{-\beta/\alpha}, 0)$ (two stable spirals for $0<\zeta<1$). $F(t)$ is the external excitation: $F(t) = f_0\cos(\omega t) + N(\sigma, \bar{x})$. Note that excitation is composed by a harmonic excitation $F(t) = f_0\cos(\omega t)$ where f_0 is the dimensionless excitation due to base acceleration ($f_0 \propto \Omega^2 X_0$ where X_0 is the dimensionless base displacement amplitude); and a random excitation $F(t) = N(\sigma, \bar{x})$, where $N(\sigma, \bar{x})$ is a Gaussian white noise with mean value $\bar{x}$ and

standard-deviation σ.

Besides two different excitations, two different systems are treated: uncontrolled and controlled systems. Controlled system has two piezoelectric elements. One is used for energy harvesting purpose, Eq. (4), and the other to provides the actuation, Eq. (5). Therefore, the equations of motion is given by:

$$\ddot{x} + 2\xi\dot{x} - 0.5x + 0.5x^3 - \chi_1 v_1 - \chi_2\left(v_2 + \frac{B_{control}}{\chi_2}\right) = f_0 \cos\Omega t, \tag{3}$$

$$\dot{v}_1 + \mu_1 v_1 + \kappa_1 \dot{x} = 0, \tag{4}$$

$$\dot{v}_2 + \mu_2\left(v_2 + \frac{B_{control}}{\chi_2}\right) + \kappa_2 \dot{x} = 0. \tag{5}$$

Concerning the controller, its design is based on two chaos control techniques: semi-continuous (SC) method (Hübinger *et al.*, 1994) and Extended Time-Delayed Feedback method (ETDF) (Socolar *et al.*, 1994).

The SC method is described by considering a discrete system of the form of a map $x^{n+1} = F(x^n, p^n)$, where $p \in \hat{A}$ is an accessible parameter for control. Let $x_C^{n+1} = F(x_C^n, p_0)$ denote the unstable fixed point on this section corresponding to an unstable periodic orbit in the chaotic attractor that one wants to stabilize. The essential idea of the controller is to monitor the system dynamics until the neighborhood of this point is reached. Then, a proper small change in the parameter p causes the next state ξ^{n+1} to fall into the stable direction of the fixed point, v_s^{n+1}. The values of scalars α and δp^n, necessary to the stabilization of system, are defined from De Paula and Savi (2011):

$$J^n \delta\xi^n + w^n \delta p^n = \alpha v_s^{n+1} \tag{6}$$

The ETDF controller requires only the information of v_2 and the control action, being given by:

$$B_{control} = K[(1-R)S_\tau - v_2],$$

$$S_\tau = \sum_{m=1}^{N_\tau} R^{m-1} v_{2_{m\tau}}. \tag{7}$$

where K and R are scalar control gains; $S_\tau = S(t-\tau)$ and $x_{m\tau} = (t - m\tau)$ are related to delayed states of the system and τ is the time delay. In general, N_τ is infinity but it can be properly defined depending on the dynamical system, here, N_τ =3.

Numerical simulations without control is carried out by considering $z = 0.01$, $c = 0.05$, $k = 0.5$ and $/ = 0.05$, the same parameters considered in Erturk *et al.* (2009) and De Paula *et al.* (2015).

RANDOM EXCITATION

Initially, consider that the energy harvesting system is subjected to random excitation. The bistable system's behavior is such that the tip of the beam can either oscillate around one equilibrium point, visiting only one well for suitable small excitations, or it can jump between the wells if the supplied mechanical energy is high enough (Ferrari *et al.*, 2010, 2011). The jumps between wells result in an average increase of the power supplied by the converter. Thus, it is interesting to define the range of excitations such that the tip oscillates around both stable equilibrium points (SEP). Figure 2 shows displacement and provided voltage with β = –2 and α =1 for $\sigma^2 = 0.64$. In this case, the tip of the beam oscillates around only one stable equilibrium point. When the excitation variance is increased to $\sigma^2 = 5.76$, the tip of the beam oscillates around both stable equilibrium points and the provided voltage increases as expected and shown in Figure 3.

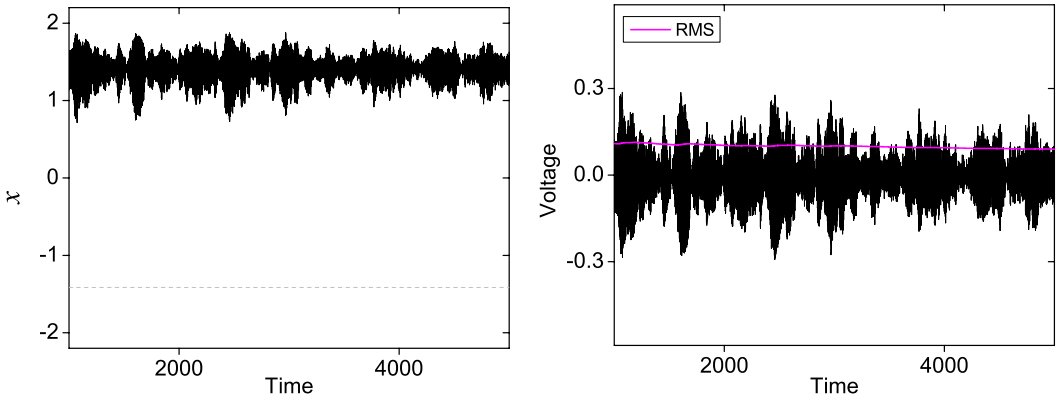

Figure 2 - Nonlinear bistable system ($U_{SEP} = -1$) response and provided voltage for $\sigma^2 = 0.64$.

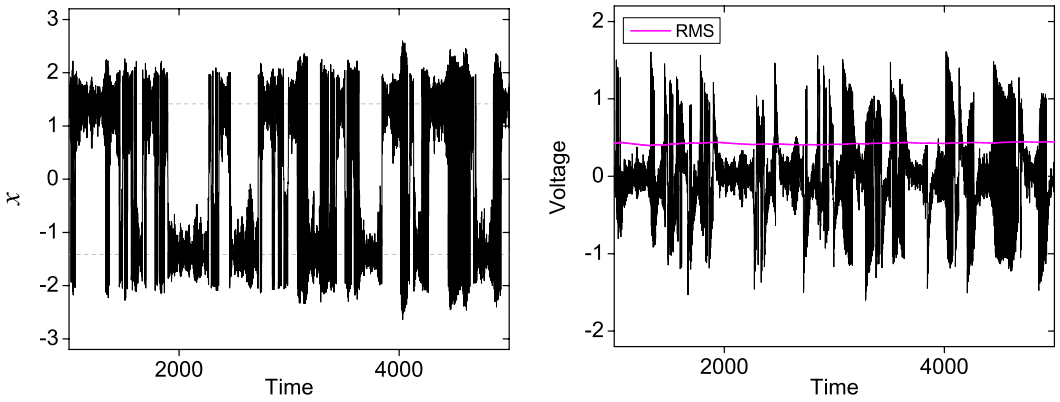

Figure 3 - Nonlinear bistable system ($U_{SEP} = -1$) response and provided voltage for $\sigma^2 = 5.76$.

A range of forcing parameter is analyzed and for each forcing variance, σ^2, simulations are carried out 50 times. The system is considered to be at rest in one of the stable equilibrium points, half of the time in each SEP. System behavior is analyzed and the percentage of times that the tip oscillates around both SEP in all 50 simulations is represented by a variable, PV_{SEP}, as presented in Figure 4. This variable is important to characterize the situation when the system presents the desired behavior that enhances the harvested energy. Due to the random excitation, the same value of f_0 can lead to different results. Hence, for the same excitation magnitude, the system can oscillate either around only one SEP or around both SEP. Three regions are defined: one region where system vibrates around only one SEP ($PV_{SEP} \leq 5\%$), called "One SEP visited"; one region where system vibrates around the two SEP ($PV_{SEP} \geq 95\%$), called "Both SEP visited"; and a transition region, where both situations can occur. From Figures 4, it is noticeable that RMS voltage of nonlinear system becomes greater than the linear system after the transition region. Thus, as verified by Ferrari *et al.* (2010, 2011) bistable system can improve the provided power, however, this happens only if the tip of the beam oscillates around both stable equilibrium points.

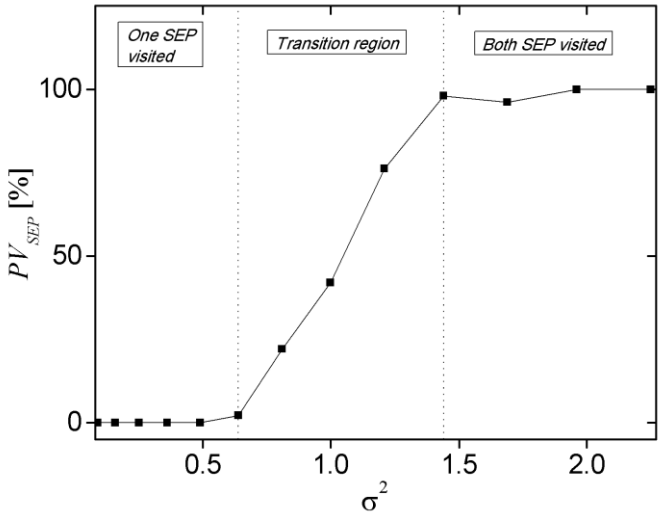

Figure 4 - Percentage of times that system vibrates around both SEP for different variances of excitation.

It should be highlighted that the transition region is centralized at $\sigma^2 = 1$. The same pattern is also observed for different values of β and α (De Paula et al., 2015). Therefore, the relation between excitation variance and stable equilibrium point potential plays an important role in system dynamics. In Figure 4, two excitation variances are highlighted: one related to the transition from "One SEP visited" to the transition region ($\sigma^2 = 0.64$) and the second when occurs at the transition from transition region to the desired behavior where system oscillates around both SEP ($\sigma^2 = 1.44$).

Figure 5 presents these two situations for different stable equilibrium point positions, x_{SEP}, (obtained by considering different values of β and α), where '♦' corresponds to the first transition while '■' corresponds to the second transition. Data obtained for each transition is fit to a third order polynomial. As mentioned before, in the situation presented in Figure 4, with β=–2 and α =1 (leading to x_{SEP}=1.4142), the first transition occurs when $\sigma^2 = 0.64$ and the second when

$s^2 = 1.44$. More details of the analysis relates to random excitation can be found at De Paula *et al.* (2015).

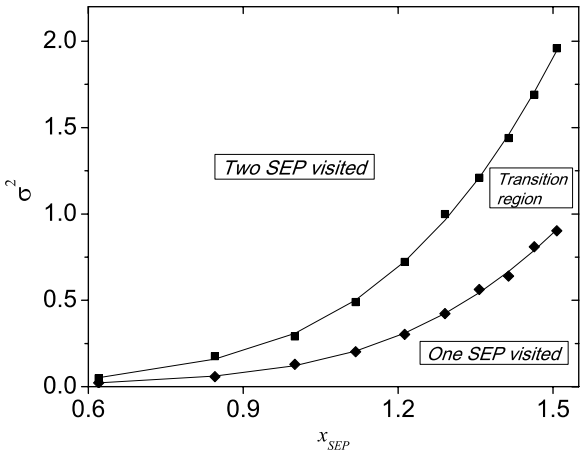

Figure 5 - Relation between excitation variance and x_{SEP} defining three regions.

HARMONIC AND RANDOM EXCITATIONS COMBINED

At this point, system is subjected to an excitation represented by a combination of harmonic and random excitations. The system performance is evaluated by considering the Power Spectral Density (PSD) that represents the distribution of power into frequency domain, as follows:

$$\hat{x}(\omega) = \int_{-\infty}^{\infty} e^{-2\pi i f t} x(t) dt \tag{8}$$

$$PSD = |\hat{x}(\omega)|^2 \tag{9}$$

where $\hat{x}(\omega)$ is the Fourier Transform. The analysis considers output and input measures, represented by the PSD of $v(t)$ and $F(t)$, respectively. They are calculated using a periodogram approach and Hanning windowing (Newland, 2005). The area under the curve is estimated for both type of excitations and represents the Power of the Signal (PS). It is established the ratio of the PS_v and PS_f as a parameter to measure the system performance, as follows:

$$r = \frac{\int_0^{\omega} PSD_v(\omega) d\omega}{\int_0^{\omega} PSD_f(\omega) d\omega} = \frac{PS_v}{PS_f} \tag{10}$$

The bigger the value of the ratio r, the larger the area under the PSD of electrical response when compared to the mechanical input. Moreover, the value of PS_{v} is related to electrical output. Thus, PS_v and r are parameters used to indicate system performance for different dynamical behaviour. The quantities $v(\mathrm{t})$ and $F(\mathrm{t})$ are dimensionless, so the PS_v and PS_f can be compared directly.

A comparison between harmonic and random excitations separately shows that harmonic excitation leads to better performance in terms of energy harvesting. In this case, different kinds of behaviors are observed, from periodic to chaotic responses. A period-1 orbit that oscillates around both stable equilibrium points is identified as the better response of the system for energy harvesting purposes. This orbit presents the bigger oscillation amplitudes from all identifies responses.

When harmonic and random excitations are combined, Noise to Signal Ratio (NSR), defined in Eq. (11), is used to quantify the level of noise in the signal.

$$NSR = \frac{\sigma}{f_0} \tag{11}$$

Figure 6 presents system response for $\beta = -2$, $\alpha = 1$, $\omega = 0.8$ and $f_0 = 0.063$, represented by the phase space (blue) and Poincaré section (magenta), and corresponding values of *PS* and *r* for different values of NSR. Note that, initially, when for small values of NSR (including situation free of noise), the system presents a period-1 orbit response that oscillates around only one stable equilibrium point. This behavior is not appropriate to energy harvesting purposes, generating low values of PS_v and *r*. When NSR is increased, after a transition region (related to the hatched part), system behavior changes considerably and a much better performance in terms of energy harvesting is achieved. By considering values of *PS* and *r*, the best performance occurs for *NSR*=1.

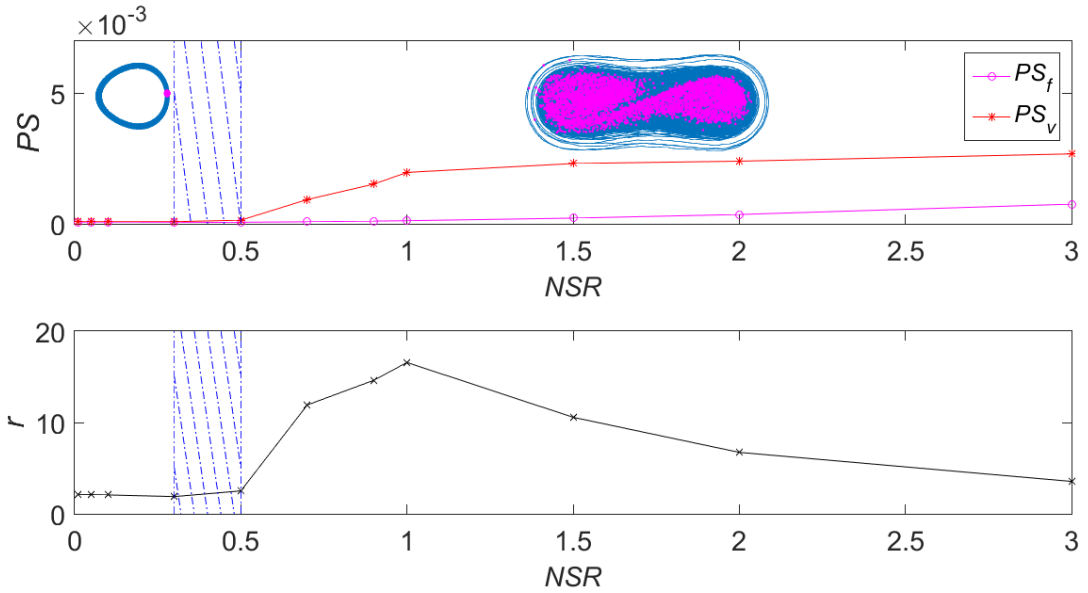

Figure 6 – System response, *PS* and *r* with ω =0.8 and f_0=0.063 for different values of NSR.

By increasing the forcing amplitude to $f_0 = 0.1$, Figure 7 presents system response, represented by the phase space (blue) and Poincaré section (magenta), and corresponding values of *PS* and *r* for different values of NSR. Note that for small values of NSR, the system presents a chaotic response. By increasing NSR, after a transition region, the system presents a response that oscillates around both stable equilibrium points with large amplitudes. This behavior presents the best performance for energy harvesting as can be observed by values of PS_v and *r*. For values of NSR > 2, another behavior is observed. By comparing this response with the chaotic one, the value of PS_v is bigger (corresponding to a better voltage output) but a smaller *r*, since more mechanical energy is provided to the system as the noise increases.

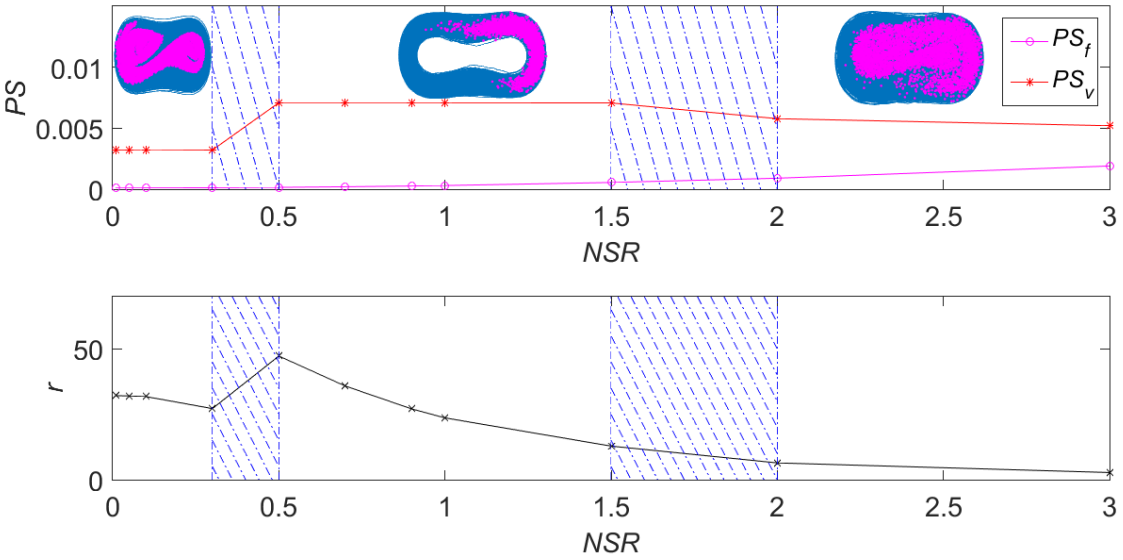

Figure 7 – System response, *PS* and *r* with ω =0.8 and f_0=0.1 for different values of NSR.

ENERGY HARVESTING AND CONTROL

At this point, piezoelectric material is used as sensor and actuator in an application simultaneously using control and energy harvesting. The chaos control is evaluated with two different aims: vibration reduction and energy harvesting. Numerical simulations are performed showing the general behavior of the harvesting-control system. Parameters shown in Table 1 are employed for all simulations. Values of ξ, χ_1, λ_1 and κ_1 are obtained from Erturk *et al.* (2009), while values of χ_2, λ_2 and κ_2 are obtained from Wang and Inman (2012). Concerning the equivalent impedance, it is adopted 112kΩ for the PZT_H circuit and 1.98MΩ for the PZT_C circuit (Wang and Inman, 2013).

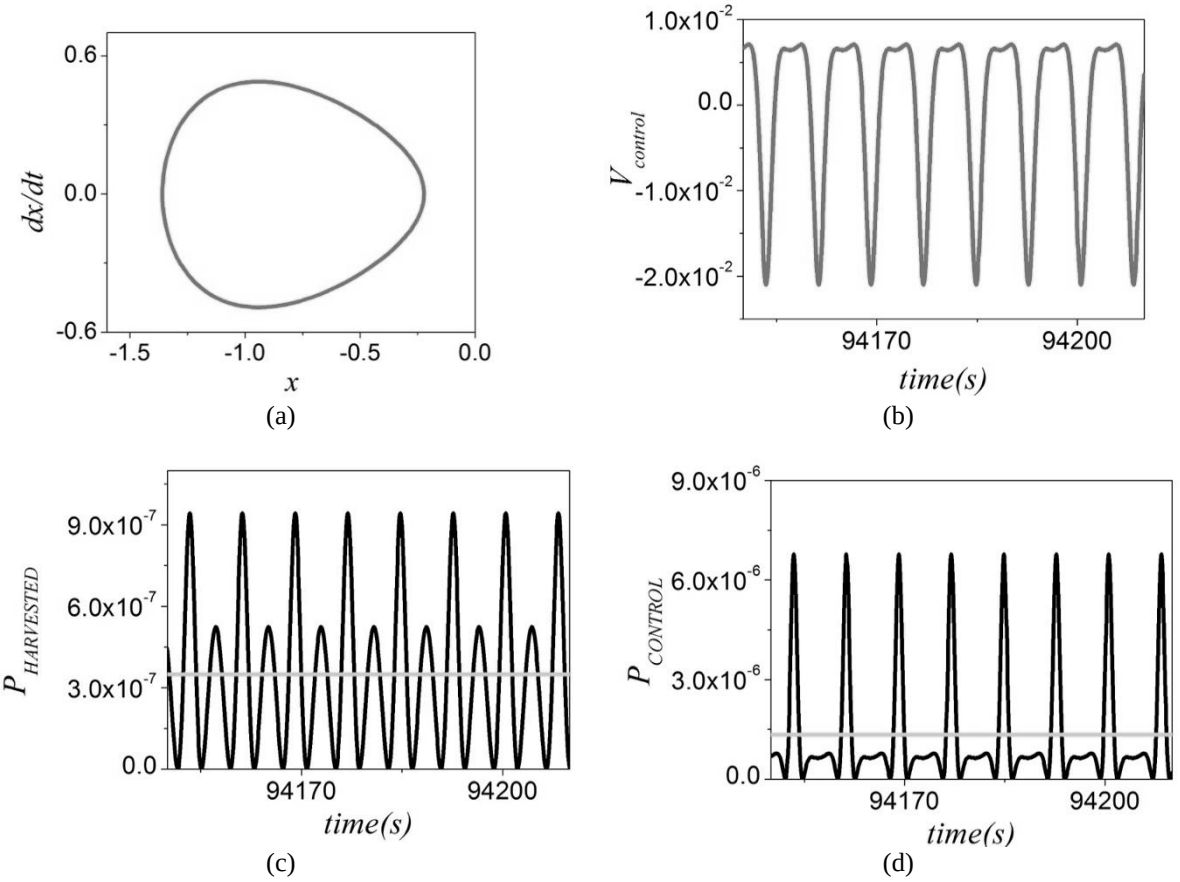

Figure 8 – ETDF method stabilization of period-1 UPO orbit with *R*=0.1 and *K*=0.6: (a) steady state phase space; (b) control signal; (c) power harvested; and (d) power consumed by the controller.

Table 1 – System parameters.

Parameters	ξ	χ_1	μ_1	κ_1	χ_2	μ_2	κ_2
Values	0.01	0.05	0.05	0.50	0.05805	-2.07596	-0.00573

Chaos control is focused on establishing a system response related to different UPOs. Initially, a period-1 UPO associated with vibration reduction purpose (response with low amplitude) is of concern. Figure 8 shows the stabilization of this UPO using ETDF method with *R*=0.1 and *K*=0.6. Steady-state phase space, control signal, instantaneous (black) and average (gray) harvested power and instantaneous (black) and average (gray) powers used by the control actuations are presented. The average electrical power consumed by the controller for the stabilization of this UPO is approximately $1.34\text{x}10^{-6}$, while the average harvested electrical power is $3.49\text{x}10^{-7}$. Hence, the piezoelectric converter provides 26% of the power consumed by the controller.

Semi-continuous (SC) controller is evaluated for the stabilization of the same UPO in order to compare its performance with ETDF. The idea is to establish a proper combination of procedures in order to obtain a better performance of the controller. Figure 9 presents results of the stabilization showing the steady-state phase space, control signal, instantaneous (black) and average (gray) harvested power and instantaneous (black) and average (gray) powers used for control actuations. The dimensionless average electrical power consumed by the controller when stabilizing the UPO is approximately 1.83×10^{-7}, while the average harvested electrical power is 3.62×10^{-7}. The net harvested power is now 1.79×10^{-7} corresponding around 14% of the harvested power obtained by the chaotic response without control. It is important to highlight that the main goal, when vibration reduction is of concern, is the use of the harvested power to supply the controller and not to use the net harvested power. Here, different from ETDF controller, the harvested power is sufficient to fully supply the controller and there is still a net harvested power. Therefore, the performance of the SC is more interesting than the ETDF since the proposed harvester-controller system presents energy autonomy.

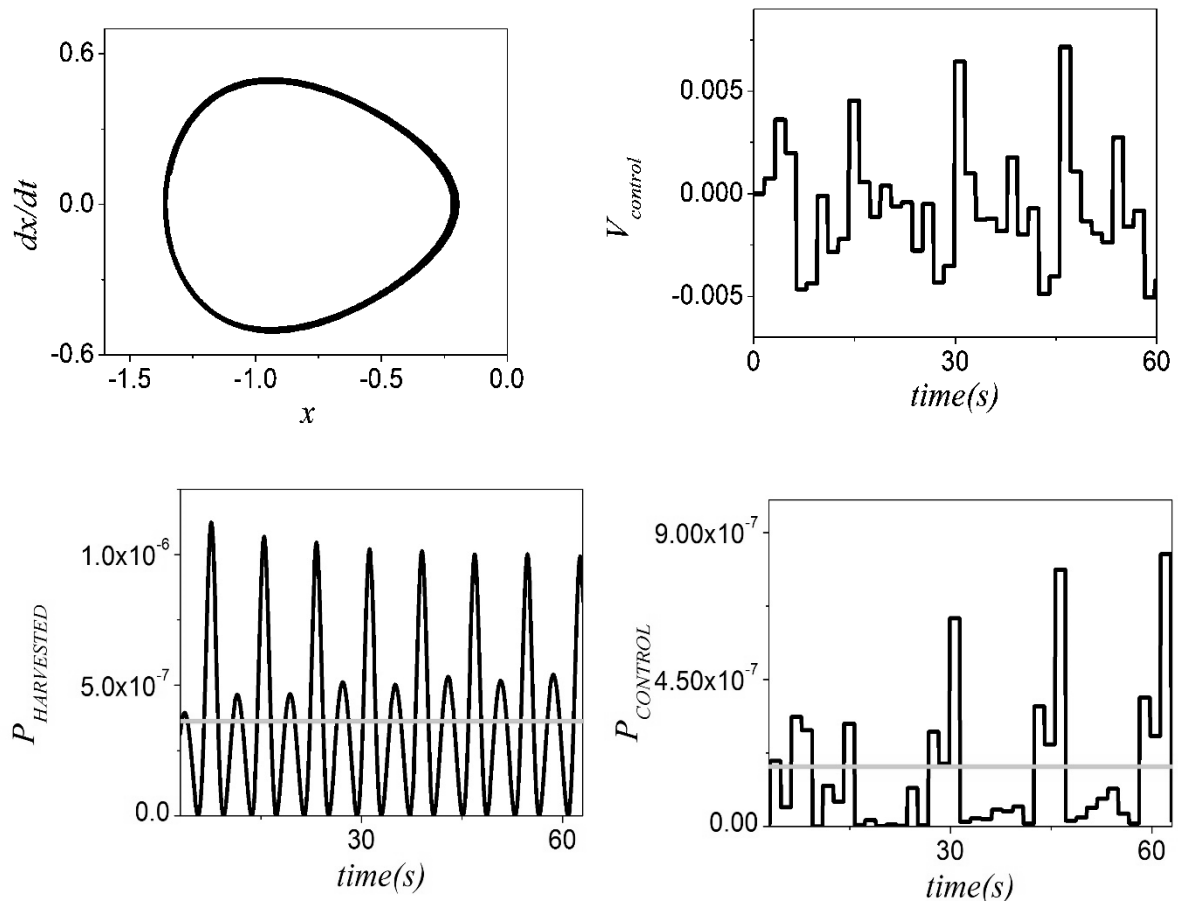

Figure 9 – SC method stabilization of period-1 UPO for energy harvesting purpose: (a) steady-state phase space; (b) control signal; (c) power harvested; and (d) power consumed by the controller.

The stabilization of a period-2 UPO associated with energy harvesting purpose (response with high amplitude) is now of concern. Figure 10 presents the stabilization of this UPO using SC method. Steady-state phase space, control signal, instantaneous (black) and average (gray) harvested power and instantaneous (black) and average (gray) power used for control actuations are presented. The dimensionless average electrical power consumed by the controller when stabilizing the UPO is approximately 2.77×10^{-7}, while the average harvested electrical power is 1.46×10^{-6}. Hence, the power generated by the piezoelectric converter is greater than the power consumed by the controller. Subtracting the average harvested power by the power consumed by the controller, one obtains 1.183×10^{-6} of net harvested power. Naturally, the available harvested power when controlling the system is smaller than when no control is considered, however, the power consumed for the stabilization is considerably smaller. Thus the periodic behavior may be more appropriate to storage energy than the chaotic response. In addition, the use of chaos control makes possible the change among several different situations, according to the needs of a given application. More details of this analysis can be found in Barbosa *et al.* (2015).

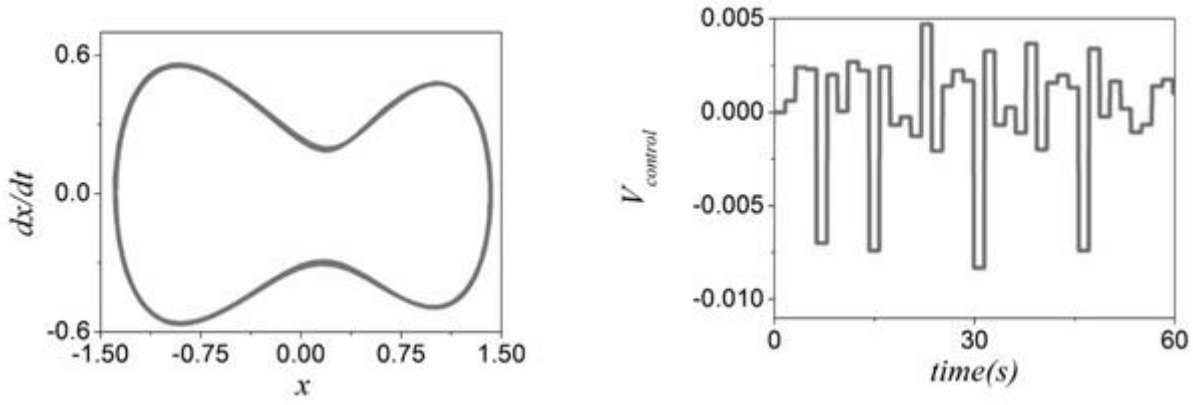

(a) (b)

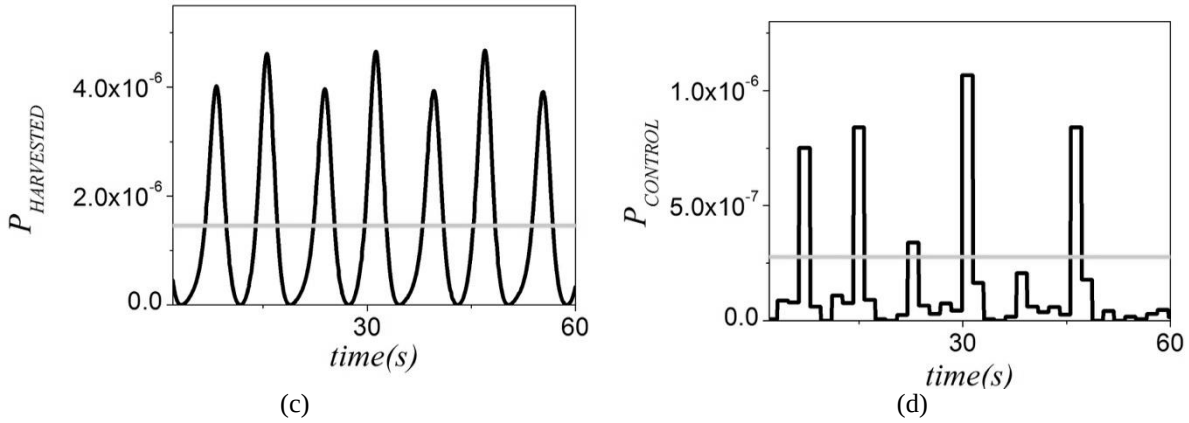

(c) (d)

Figure 10 – SC method stabilization of period-2 UPO for energy harvesting purpose: (a) steady-state phase space; (b) control signal; (c) power harvested; and (d) power consumed by the controller.

CONCLUSIONS

Piezoelectric vibration-based energy harvesting is treated considering different situations. A nonlinear piezomagnetoelastic generator represented by a bistable Duffing-type oscillator is investigated. Initially, an analysis of the voltage provided by random excitations is carried out. Variance defines energy harvesting enhancement. There is a relation quantified for a variety of different stable equilibrium point positions, showing a trend between the excitation and stable equilibrium point. Three regions are defined: one region where the tip of the beam oscillates around only one stable equilibrium point; the desired region where system jumps from one stable equilibrium point to the other; and a transition regions between these two behaviors. The transition between these three regions is clearly observed, defining the desired region of oscillation. This analysis can be useful in the design of energy harvesting system under random excitation. Thus, for a given bistable piezoelectric generator, it is possible define the minimum excitation variance that enhances the harvested energy. Similarly, if a given excitation is provided, it is possible to define bistable system characteristics that enhance the harvested energy. The second analysis considers the same system subjected to a combination of harmonic and random excitations. A methodology to evaluate the system performance, that combines determinist and non-deterministic excitations, is proposed and more appropriate behaviors for energy harvesting can be specified. Results show that introduction of noise in the harmonic excitation can improve system performance and the proposed methodology can be used to define appropriate operational regions. Finally, piezoelectric materials are used as sensor and actuator for control purposes. The main idea is to exploit the system flexibility in order to change from various desired UPOs embedded in a chaotic attractor. In addition, controller power can be fully or partially provided by the energy harvesting system. In this regard, two goals are considered: vibration reduction and energy harvesting. Two control methods are employed allowing a combination for UPO stabilization purposes: Extended Time-Delay Feedback (ETDF) and semi-continuous (SC). The UPO stabilization can define several interesting situations. Some of them imply a vibration reduction and the controller power supply is provided partially or fully by the power harvester, depending on the chaos control technique employed. Some other situations, related to higher vibration amplitudes, can provide the whole power needed for the controller and the net harvested power can be used for other energy harvesting purposes. Therefore, the combination of chaos control and energy harvesting system can be useful for different situations, especially because the controller requires low power of the order provided by the energy harvesting component.

REFERENCES

Barbosa, W. O. V. ; De Paula, A. S. ; Savi, M. A. ; Inman, D. J. . Chaos control applied to piezoelectric vibration-based energy harvesting systems. The European Physical Journal. Special Topics, v. 224, p. 2787-2801, 2015

Cottone, F.; Vocca, H.; Gammaitoni, L. (2009) "Nonlinear energy harvesting", *Physical Review Letters*, v.102, p.080601, 4 pages.

De Paula, A. S.; Inman, D. J. ; Savi, M. A. (2015), "Energy harvesting in a nonlinear piezomagnetoelastic beam subjected to random excitation", *Mechanical Systems and Signal Processing*, v. 54-55, p. 405-416.

De Paula, A. S. and Savi, M. A. (2011), "Comparative analysis of chaos control methods: a mechanical system case study", *International Journal of Non-linear Mechanics*, v.46, n.8, pp.1076-1089, 2011.

Erturk, A. and Inman, D. J. (2008), "A Distributed Parameter Electromechanical Model for Cantilevered Piezoelectric Energy Harvesters", ASME J. Vibr. Acoust., v.130, 041002.

Erturk, A. and Inman, D. J. (2009), "An experimentally validated bimorph cantilever model for piezoelectric energy harvesting from base excitations", Smart Materials and Structures, v. 18, 025009.

Erturk, A., Bilgen, O.; Inman, D. J. (2008), "Power generation and shunt damping performance of a single crystal lead magnesium niobate-lead zirconate titanate unimorph: Analysis and experiment", Appl. Phys. Lett., v. 93, 224102.

Erturk, A.; Hoffmann, J.; Inman, D.J. (2009), "A piezomagnetoelastic structure for broadband vibration energy

harvesting", Appl. Phys. Lett., v.94, 2541102(3 pages).
Ferrari, M.; Baù M.; Guizzetti, M.; Ferrari, V. (2011), "A single-magnet nonlinear piezoelectric converter for enhanced energy harvesting from random vibrations", Sensors and Actuators A: Physical, v. 172, pp.287-292.
Ferrari, M.; Ferrari, V.; Guizzettia, M.; Andòb, B.; Bagliob, S.; Trigonab, C. (2010) "Improved energy harvesting from wideband vibrations by nonlinear piezoelectric converters ",Sensors and Actuators A: Physical, v. 162, pp.425-431.
Newland, D.E. (2005). *An Introduction to Random Vibrations, Spectral & Wavelet Analysis*: Third Edition (Mineola, N.Y: Dover Publications).
Pyragas, K. (1992), "Continuous control of chaos by self-controlling feedback", *Phys. Lett. A*, v.170, pp.421-428.
Shahruz, S.M. (2008) Increasing the efficiency of energy scavengers by magnets, *Journal of Computational and* Nonlinear Dynamics, v.3, p. 041001, 12 pages.
Wang, Y. and Inman, D. J. (2013), "Experimental Validation for a multifunctional Wing Spar With Sensing, Harvesting, and Gust Alleviation Capabilities", *IEEE/ASME Transations on Mechatronics*, v. 18, n. 4, p.1289-1299.
Wang, Y. and Inman, D. J. (2012), "Simultaneous energy harvesting and gust alleviation for a multifunctional composite wing spar using reduced energy control via piezoceramics", *Journal of Composite Materials*, v.47, n.1, p. 125–146.

RESPONSIBILITY NOTICE

The authors are the only responsible for the material included in this paper.